Vol. 506: 15–30, 2014
doi: 10.3354/meps10777

MARINE ECOLOGY PROGRESS SERIES
Mar Ecol Prog Ser

Published June 23

Effect of nearshore surface slicks on meroplankton distribution: role of larval behaviour

Nicolás Weidberg[1,4,*], Carla Lobón[1], Eva López[1], Lucía García Flórez[2], María del Pino Fernández Rueda[2], John L. Largier[3], José Luis Acuña[1]

[1]Área de Ecología. Dpto. Biología de Organismos y Sistemas de la Universidad de Oviedo, C/ Valentín Andrés Álvarez s/n, 33071 Oviedo, Asturias, Spain

[2]Centro de Experimentación Pesquera, Escuela de Formación Profesional Náutico-Pesquera, Avenida Príncipe de Asturias s/n, 33212 Gijón, Asturias, Spain

[3]Bodega Marine Laboratory, University of California, Davis, 2099 Westside Drive, Bodega Bay, 94923-0247 California, USA

[4]*Present address:* Coastal Research Group, Department of Zoology and Entomology, Artillery Road 6140, Rhodes University, Grahamstown, South Africa

ABSTRACT: During a 10 d survey off the Central Cantabrian Coast, we used GPS-drifters and bongo nets to observe water circulation and meroplankton distributions associated with 4 different nearshore surface slicks or foam lines. Accumulation of larvae was observed associated with surface convergence at these slicks. Three of the slicks moved onshore at velocities ranging between 2 and 11 cm s^{-1} and accumulated cyprid barnacle larvae, crab zoeae, littorinid veligers, and annelid and ascidian larvae from the onshore side of the front. The predominant onshore source of larvae suggests that, in our study area, surface slicks may result in onshore retention of larvae. Accumulation at surface slicks was greatest for larvae with swimming speeds about half the speed of the cross-frontal, horizontal surface convergence. We hypothesize that this peak corresponds to an optimum slick speed for which the horizontal surface flow is strong enough to bring significant numbers of larvae to the front, but the associated downward vertical flow at the convergence line is weak enough to be countered by upward swimming. However, we estimated that the vertical flow may be stronger than the horizontal convergence, thus buoyancy and behavioural shifts in larval swimming performance may play an important role in the frontal accumulation of larvae. Given differences in swimming capabilities of different taxa and larval stages, a surface convergence can bring about different transport outcomes, accumulating or acting as a barrier for some larvae while allowing others to move through.

KEY WORDS: Meroplankton · Coastal fronts · Convergence currents · Swimming velocity

INTRODUCTION

Meroplankton distribution is of great importance in the dynamics of coastal populations (Sandifer 1975, Gaines & Roughgarden 1985, Largier 2002, 2003, Shanks et al. 2002, Becker et al. 2007, Pineda et al. 2007, 2009). Although many studies have inferred patterns in abundance and recruitment from offshore sampling surveys, attention has shifted recently to nearshore waters (McCulloch & Shanks 2003, Shanks et al. 2003, Pineda et al. 2007, Morgan et al. 2010), the dynamics of which govern larval spawning and recruitment (Guichard & Bourget 1998, Archambault & Bourget 1999).

One of the most evident hydrographic features in nearshore waters is the presence of foam lines or lines of oily surface waters called slicks. These slicks indicate convergent surface flow usually occurring at fronts, which are the boundary between different water types and thus characterized by horizontal sur-

*Corresponding author: j_weidberg@hotmail.com

face gradients of physicochemical properties (Le Fevre 1986, Longhurst 1998). Surface slicks can occur on a variety of scales associated with flow–topography interactions, tidal mixing, wind patterns and land runoff, but they can also be observed as propagating features associated with internal waves (e.g. Romano 1995, Leichter et al. 1998, McCulloch & Shanks 2003, Shanks et al. 2003). Irrespective of their physical origin, frontal structures that exhibit a foam line or surface slick are characterized by a convergence in surface flow and associated subduction in which upward-swimming or buoyant organisms and objects may accumulate, provided that their upward velocity is faster than the downward movement of water (Franks 1992, Largier 1993, Pineda 1999, Helfrich & Pineda 2003, Shanks & Brink 2005, Scotti & Pineda 2007).

The effect of slicks has been studied in many groups of organisms (e.g. Kingsford & Choat 1986, Young & Adams 2010) but rarely in meroplankton (but see Shanks 1995 and Pineda 1999). Here, the swimming abilities of the different larval taxa are shown to relate to the strength of accumulation at the front, although even very slow swimming larvae like gastropod veligers, that attain speeds of a few mm s^{-1}, can resist typical vertical flows (Poulin et al. 2002, Shanks & Brink 2005). Similar abilities have been demonstrated for the whole zooplankton community (Genin et al. 2005). Because of the weak swimming abilities of medium-sized zooplankters, they have traditionally been considered passive tracers of surface frontal circulation (Mann 1988), although there are a few studies pointing to the possibility that larvae could control their position in the horizontal plane (Luckenbach & Orth 1992, Abelson 1997, Metaxas 2001). Weak swimming capabilities have been included in theoretical models to explore spatial distributions of larvae around fronts (e.g. Franks 1992) and have also been invoked to qualitatively explain cross-frontal abundance patterns in the field (Pineda 1999, Shanks et al. 2000). For population dynamics, it is not only the presence of fronts that matters, but also how factors like frequency of occurrence, strength of convergent flow and persistence of the front interact with factors such as age, size and swimming behaviour of larvae (Largier 1993).

Here we present detailed observations of the structure and dynamics of 4 slicks off the coast of Cudillero in northern Spain, along with the distribution of meroplanktonic taxa in the vicinity of these fronts at an unusually fine sampling scale of a few tens of meters. The spatial, temporal and taxonomic resolution of our study has allowed us to characterize the convergent flow at the fronts, to measure the strength of larval accumulation for different species at the fronts and infer their source (onshore or offshore waters). In addition, we relate the potential for accumulation of larvae to the swimming abilities of the different taxa and the strength of the surface convergence. To our knowledge, this study represents the first attempt to relate locomotion abilities of the organisms to observed distributions across convergences associated with nearshore fronts.

MATERIALS AND METHODS

This study was conducted from 14 to 24 June 2009 at a site close to the Cudillero Harbour (Fig. 1), where slicks were frequently observed (Weidberg et al. 2013). Hourly wind speed and direction data were

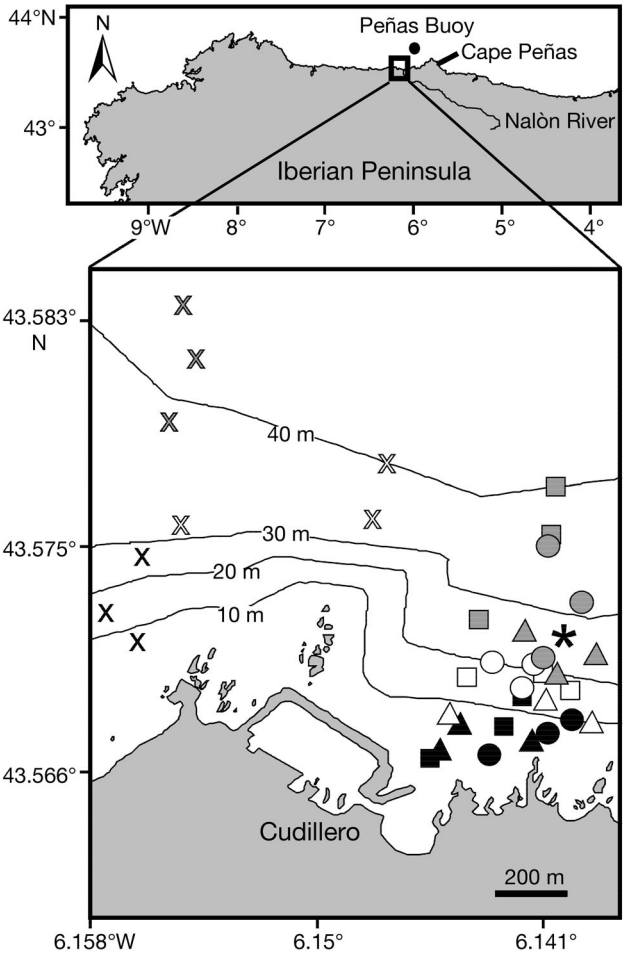

Fig. 1. Study site. Circles, crosses, squares and triangles stand for stations sampled at Front 1 to 4, respectively; the asterisk shows the position of the ADCP current meter. Symbol shades represent positions with respect to the front: on shore (black), at the front (white) and offshore (grey)

measured at the moored Peñas Buoy (Fig. 1; www.indicedeafloramiento.ieo.es/index1_en.php), which has been used to describe the local meteorological conditions in previous studies (Rodríguez et al. 2011). We used these variables to calculate the upwelling index according to Bakun (1973).

For each front, we first looked from the boat for foam lines or linear slicks at the surface. If more than one was present, we selected the most conspicuous one. Physicochemical variables and meroplankton were then sampled from the 9 m long boat 'Nueva Asturias', and a drifter experiment was conducted simultaneously from an inflatable, 4.5 m motorboat. Within a period of less than 3 h, we conducted CTD casts and zooplankton bongo tows at 3 stations at the front, 3 stations landward (inshore side) and 3 stations seaward (offshore side) of the front (Fig. 1). We alternated CTD casts and tows at frontal, offshore and onshore sites, because slicks could disappear before completing a set of observations. A SBE-25 or SBE-19 CTD package was deployed at each of the 9 stations to obtain vertical profiles of salinity, temperature, density and chlorophyll fluorescence. The average time interval between CTD casts was 10 min. Distances from offshore and onshore stations to the front varied from 10 to 600 m. Contour plots of hydrographic structure across the front were generated with the Surfer 8 software package. Given the rapid movement and deformation of these structures, the distances in these representations can only be considered approximate.

Drifter experiments

At each slick and concurrently with our sampling survey, we deployed a set of 15 GPS-tracked surface drifters inspired by the design of Magome et al. (2007). They consisted of a square styrofoam float with a wooden board (0.025 m^2), which was hung at 0.45 m depth from a rope and was kept taut by a weight to an underwater sail. Each drifter was marked with a coloured flag to distinguish those deployed in a linear pattern along the front from those inshore of the front and those offshore of the front (n = 5 at each location). Each drifter was equipped with a BT-Q1000X QSTARZ data-logging GPS unit located inside a plastic box and set to record the position every 3 s. Drifter experiments lasted 15 to 90 min depending on the proximity to the coast, the persistence of the front and the weather conditions. Drifter trajectories were plotted using ArcGis 9 software. We approximated the shape of the front by the line of drifters that were deployed in the front at the beginning of each drifter experiment. We then projected a line perpendicular to the front, which we used as reference to calculate the velocity component perpendicular (Y-component) and parallel (X-component) to the front for offshore drifters (μY_{off}, μX_{off}), onshore drifters (μY_{on}, μX_{on}) and drifters at the front (μY_f, μX_f) in cm s^{-1}. These velocities were obtained for each drifter by dividing displacement along and across the line perpendicular to the front by travel time. We paid special attention to observe and log which drifters entered the front from which side and which drifters did not remain inside the front.

Meroplankton sampling

We used a bongo net (100 µm mesh size, 2.4 m length, 20 cm radius) equipped with flow meters and floats to sample meroplankton within the upper 20 cm of the water column. Length and width of both the cylindrical and conical parts of the net were especially designed to avoid clogging in high-chlorophyll coastal waters (Sameoto et al. 2000). The net was towed after each CTD cast at 2 to 3 knots (1.03 to 1.54 m s^{-1}) for 3 min, in a tight circle around the station (when outside the foam line) or along the foam line. Thus, we obtained 9 tow samples per front, 3 at each position with respect to the front (onshore, offshore and at the front). It was usually difficult to steer the boat so that the net remained within the meandering geometry of the front, thus larval densities may be underestimated at the front. Samples were preserved in 4% formalin with seawater in 250 ml bottles. We examined 10% aliquots from all the samples except from those collected at the fronts, where we examined 5% due to the high larval concentrations. As we selected only the most common organisms for the statistical analyses, this difference in percentage is not expected to yield significant differences in the calculation of total abundances. All meroplankton were identified to the lowest possible taxonomic level, including stages in some of the cases. When presenting larval abundance results, we ordered the taxa according to larval swimming velocities reported in the literature.

Data analysis

Detection of accumulation patterns. We used an ANOVA design with 1 fixed factor (location with

respect to the front) and 3 levels: offshore, inshore or frontal. As dependent variable we used the larval abundance of each taxon independently, with L_{off}, L_{on} and L_f standing for larval abundances offshore of the front, onshore and at the front in individuals m^{-3}, respectively. To avoid heterogeneity of variances, we used log-transformed abundances. For analysis, we only used those taxa that exhibit concentrations of at least 10 individuals m^{-3} at one of the stations. If there was a significant effect of the fixed factor, we conducted post hoc Fisher LSD contrasts. We considered 3 potential situations: frontal accumulation (higher abundances in the front with respect to both sides), onshore aggregation (onshore or both onshore and frontal abundances were higher), and offshore aggregation (offshore or both offshore and frontal abundances were higher).

Sources of accumulation. To infer which side of the front was the source of larvae accumulating at the front, we modified the method of Pineda (1999). First, we calculated the absolute velocities along a direction perpendicular to the front of the frontal (μY_f), offshore (μY_{off}) and onshore (μY_{on}) waters. In contrast to Pineda (1999), who was studying convergence associated with propagating internal waves, we could observe movement towards the front from either side. Surface convergence was thus calculated as:

$$\begin{aligned} \Delta\mu Y_{off} &= \mu Y_{off} - \mu Y_f \\ \Delta\mu Y_{on} &= \mu Y_f - \mu Y_{on} \end{aligned} \quad (1)$$

where $\Delta\mu Y_{off}$ and $\Delta\mu Y_{on}$ denote the velocities of offshore and onshore surface waters towards the front in m s^{-1}, respectively (Table 1). Larval supply rates to the front from onshore (S_{on}) or offshore (S_{off}) sides of the front (larvae m^{-2} s^{-1}) could thus be calculated as:

$$\begin{aligned} S_{off} &= \Delta\mu Y_{off} \times L_{off} \\ S_{on} &= \Delta\mu Y_{on} \times L_{on} \end{aligned} \quad (2)$$

where L_{off} and L_{on} are larval densities at the offshore and the onshore sides of the front, respectively. Comparison between S_{off} and S_{on} provides an indication of the source of the larvae accumulating at a front. Inferring larval sources from these supply rates has obvious limitations: if both relative speeds $\Delta\mu Y_{off}$ and $\Delta\mu Y_{on}$ are positive and larvae do not concentrate significantly at the front, it means that the larvae sink in the convergence and cross the front. In this case, larval abundances on one side could be dependent on the supply rate from the other, so it does not make sense to make any comparison.

Along-frontal and vertical flows. Accumulation of larvae at the front is a sum of flux convergence in all 3 dimensions of space (a 3-dimensional mass-balance), i.e. including convergent or divergent fluxes in the along-front and vertical directions. Thus, where a net perpendicular flow was detected ($\Delta\mu Y > 0$), relative along-frontal speeds were calculated as:

$$\begin{aligned} \Delta\mu X_{off} &= \mu X_{off} - \mu X_f \\ \Delta\mu X_{on} &= \mu X_f - \mu X_{on} \end{aligned} \quad (3)$$

This procedure allowed the calculation of the vertical component of the flow (μZ) by taking into account the 3-dimensional mass balance:

$$\Delta\mu X/L + \Delta\mu Y/W + \Delta\mu Z/H = 0 \quad (4)$$

And with $\mu Z = 0$ at the surface, at depth H we obtained:

$$-\mu Z = \Delta\mu X \times H/L + \Delta\mu Y \times H/W \quad (5)$$

where H is the depth of convergent horizontal flow tracked by surface drifters, W is the width of the surface convergence zone (distance between drifters used to calculate $\Delta\mu Y$), and L is distance between drifters used to calculate $\Delta\mu X$. In the absence of vertical profiles of flow velocity, the ratios H/W and H/L could not be adequately quantified and were assumed to be equal to 1 in subsequent calculations.

Accumulation and velocity ratios. Once the source of larvae was known, a simple accumulation ratio (A) could be calculated following Pineda (1999):

$$A = L_f/L_s \quad (6)$$

where L_f and L_s are larval concentration at the front and in the source water, respectively. L_s can be equal to L_{off} or L_{on}, depending on whether the source is the offshore or the onshore side of the front.

For a given front, we expected accumulation of larvae carried towards the front that are capable of swimming against the vertical currents associated with the surface convergence at the front, and which are not removed from the front by flows at depth. Thus, larval accumulation A could be expected to depend on the swimming ability of the zooplankter μ_l relative to both the cross-frontal and vertical flows which we quantified as:

$$Q_Y = \mu_l/\Delta\mu Y_s \text{ and } Q_Z = \mu_l/\mu Z_s \quad (7)$$

where μ_l is the swimming velocity of larvae as reported in the literature and $\Delta\mu Y_s$ and μZ_s are the cross-frontal and vertical convergences on the side of the slick from which larvae are sourced, i.e. $\Delta\mu Y/\mu Z_s = \Delta\mu Y/\mu Z_{off}$ or $\Delta\mu Y/\mu Z_s = \Delta\mu Y/\mu Z_{on}$, depending on the source of larvae. Similar ratios have been used to characterize the role of plankton behaviour (Gallager et al. 2004). Q_Y and Q_Z indicate whether the larva is

faster ($Q_Y > 1$, $Q_Z > 1$) or slower ($Q_Y < 1$, $Q_Z < 1$) than the velocity of the cross-frontal and vertical flows, respectively. As we hypothesized that frontal accumulation may develop at intermediate levels of these velocity ratios (strong enough to transport larvae towards the front in significant amounts but weak enough to avoid subduction once there) we used simple quadratic models to fit the accumulation ratio data set.

RESULTS

Structure of the water-column

We observed and sampled 4 fronts between 15 and 24 June 2009. Front 1 occurred in the afternoon of 15 June approx. 500 m off the coast. The wind had been weak and variable during the preceding 3 d, with brief episodes of positive Ekman transport (Fig. 2). The foam line of Front 1 coincided with a clear hydrographic cross-shore gradient, with salinity and density decreasing seawards from 35.6 to 32 psu and from 26.6 to 22.8 kg m^{-3}, respectively, while fluorescence increased from 1 to 9 arbitrary units (a.u.; Fig. 3). We observed marked thermal stratification in waters deeper than 20 m on the offshore side of the front, and shoaling of cool, high-fluorescence waters, consistent with upwelling or internal-wave run-up effects (Fig. 3).

Front 2 occurred in the morning of 21 June approx. 500 m from the coastline. It was a straight foam line with a noticeable accumulation of floating algae and debris. We sampled this front during strong northeasterly winds (~8 m s^{-1}) and offshore Ekman transport of more than 1000 m^3 km^{-1} s^{-1}. Around the time of sampling, wind and Ekman transport varied daily due to the sea–land breeze (Fig. 2). Front 2 was the only sampled front that did not reach the shore and instead started to disintegrate 20 min after the beginning of sampling. The convergence was not associated with strong cross-shore gradients in the main hydrographical variables (Fig. 3). Although cooler water was observed upwelling on the inshore side of the front, it did not create any notable density gradient (Fig. 3).

Front 3 occurred in the afternoon of 23 June approx. 250 m offshore during weak winds (~2 m s^{-1}) from the southwest and after 4 d of relatively strong upwelling (Fig. 2). CTD profiles showed a warm, low-fluorescence surface layer with a low-salinity lens in the vicinity of the front (Fig. 3). The thermocline was <10 m deep and did not rise at the coast, although contour lines of temperature, salinity and density outcropped locally at the front. Immediately below the thermocline was a sub-surface chlorophyll maximum, at 10 to 15 m (Fig. 3).

Front 4 occurred on the morning of 24 June at 350 m off the coast. It was the most visually evident and active front, with a wide foam line that accumulated floating debris, attracting feeding fish and

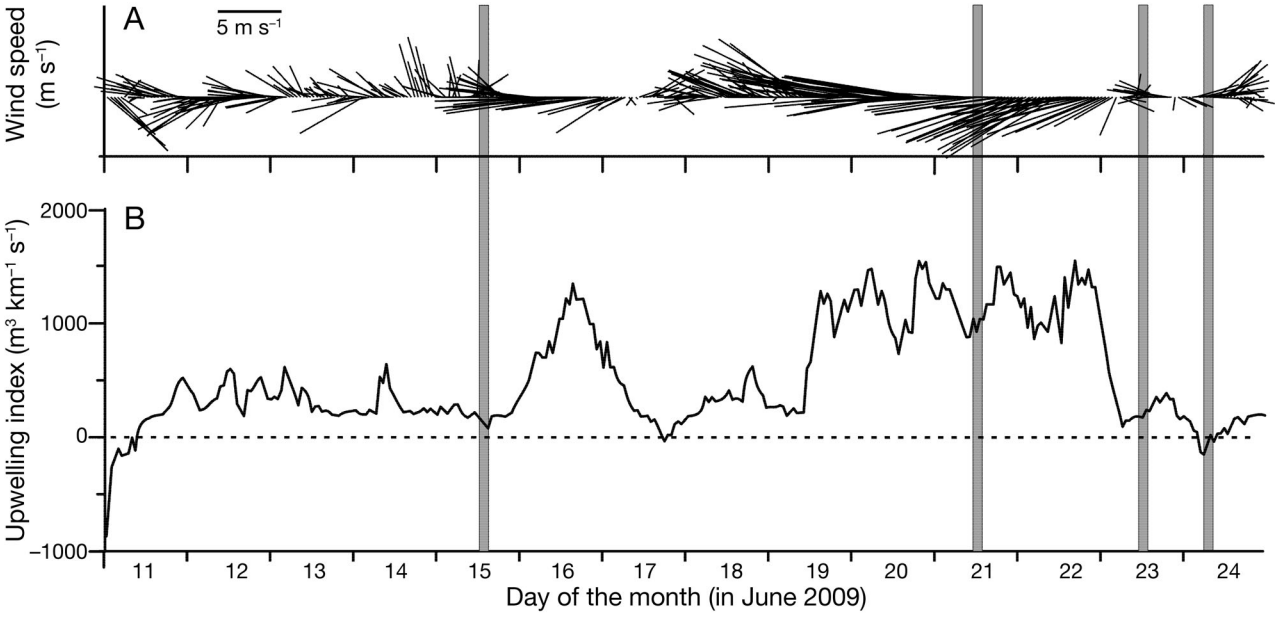

Fig. 2. (A) Hourly time series of wind vectors and (B) upwelling index from 11 to 24 June 2009. Grey bars highlight the sampling times for the 4 fronts. Wind vectors (m s^{-1}) are in the direction of the wind, with upwards vectors indicating winds blowing from the South

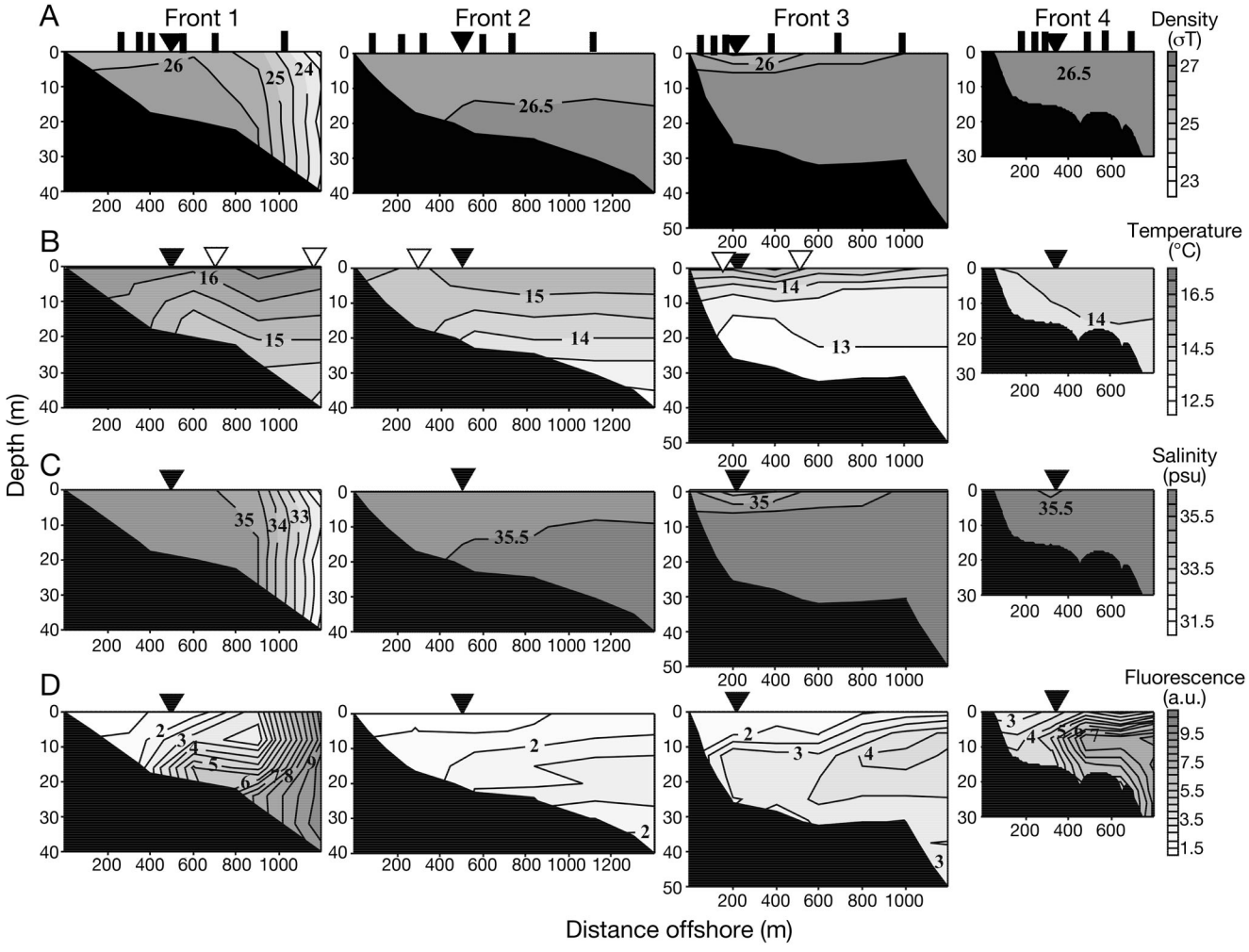

Fig. 3. Profiles of (A) density, (B) temperature, (C) salinity and (D) fluorescence for each front. Dark and white triangles mark the initial mean position of the front and the location of vertical deformations in the thermocline, respectively. Dark bars indicate the positions of the CTD casts. Black area is sea bottom

seagulls. The CTD profiles at this front were characterized by nearly homogeneous density with weak thermal stratification and a small lens of low-salinity water at the front. We found a clear gradient in fluorescence, which increased rapidly from 3 to 7.5 a.u. (similar to Front 1, but without the low-salinity plume; Fig. 3).

Flow patterns

Front 1 displayed the most complex water circulation patterns. During the 80 min observation, 4 out of 5 drifters deployed at the front moved with the front as it was displaced southeast and toward the shore at a speed of $\mu Y_f = 3.8 \pm 0.6$ cm s^{-1} (Table 1, Fig. 4). The front reached the coast about 3 h after the beginning of sampling. During the observation period, the foam line weakened and became less clear. All onshore drifters moved toward the front at $\mu Y_{on} = -4.8 \pm 1.4$ cm s^{-1} (Table 1, Fig. 4). After reaching the front, they experienced a clear change in their trajectories and moved with the foam line to the east at speeds of 3.4 cm s^{-1} (Table 1). Convergence cross-frontal velocity at the onshore side was thus $\Delta\mu Y_{on} = 8.6$ cm s^{-1}, the highest observed in our study, yielding to high downwelling speeds of 9.5 cm s^{-1} (Table 1). The trajectories of the offshore drifters were more variable, slightly westward and did not converge on the front, with $\Delta\mu Y_{off} < 0$ cm s^{-1} (Table 1, Fig. 4).

Flow patterns around Front 2 were much simpler: all drifters moved slowly westwards and toward the coast (Table 1, Fig. 4). In the direction perpendicular to the front, onshore drifters moved slightly more

Table 1. Mean (±SD) absolute (μ) and relative (Δμ) velocities (cm s^{-1}) of surface waters moving perpendicular (Y-direction) or parallel (X-direction) to the front. Water movements were recorded on the onshore side of the front ($_{on}$), at the front ($_{f}$), or on the offshore side ($_{off}$). In addition, a vertical flow component Z was calculated. Positive values indicate southwards, eastwards and upwards directions on Y, X and Z axes, respectively. na = not applicable calculation (in the absence of cross-frontal convergence, i.e. $\Delta\mu Y < 0$). See 'Materials and methods: Data analysis' for definitions and measurement of the variables

	μY_{on}	μY_{f}	μY_{off}	$\Delta\mu Y_{on}$	$\Delta\mu Y_{off}$	μX_{on}	μX_{f}	μX_{off}	$\Delta\mu X_{on}$	$\Delta\mu X_{off}$	μZ_{on}	μZ_{off}
Front 1	−4.8 ± 1.4	3.8 ± 0.6	1.5 ± 0.6	8.6	−2.3	2.5 ± 2.6	3.4 ± 0.4	−2.2 ± 4	0.9	na	−9.5	na
Front 2	2.0 ± 0.5	2.5 ± 1.5	1.8 ± 0.4	0.5	−0.7	−9.8 ± 2.0	−7.3 ± 0.3	−7.8 ± 0.8	−2.4	na	1.9	na
Front 3	9.4 ± 0.9	10.9 ± 0.1	6.4 ± 0.6	1.5	−4.5	13.6 ± 2.1	19.4 ± 1.7	22.9 ± 1.4	5.7	na	−7.2	na
Front 4	−3.5 ± 0.2	2.0 ± 0.4	8.3 ± 0.4	5.5	6.3	4.1 ± 1.9	8.2 ± 0.8	6.2 ± 0.8	4.1	−2	−9.6	−4.2

slowly than those deployed in the front (2 ± 0.5 and 2.5 ± 1.5 cm s^{-1} respectively; Table 1, Fig. 4), accounting for a weak convergence on the onshore side ($\Delta\mu Y_{on}$ = 0.5 cm s^{-1}; Table 1). However, given that onshore waters moved faster to the west than those within the front ($\Delta\mu X_{on}$ = −2.4 cm s^{-1}; Table 1), such weak convergence caused upward instead of downward flow at the front (μZ_{on} = 1.9 cm s^{-1}; Table 1). Offshore drifters did not converge on the front but instead moved with it ($\Delta\mu Y_{off}$ slightly negative). Although the front was no longer visible after 20 min, drifter trajectories did not change appreciably over the observation period.

Front 3 was the most active in terms of drifter velocities (Fig. 4). All drifters moved rapidly towards the coast and eastwards (Table 1). However, $\mu Y_{off} < \mu Y_{f}$ (Table 1), and the offshore drifters never reached the front (Fig. 4). Visual inspection indicated that only one of the drifters deployed right at the front stayed with the fast-moving slick line (μY_{f} = 10.9 ± 0.1 cm s^{-1}; Table 1), while the rest of them were slowly left behind. The onshore drifters, moving at 9.4 ± 0.9 cm s^{-1}, were almost reached by the front by the time they reached the coast (Fig. 4). This indicates a slow convergent flow at the onshore side of the front ($\Delta\mu Y_{on}$ = 1.5 cm s^{-1}; Table 1), which led to vertical subduction (μZ_{on} = −7.2 cm s^{-1}; Table 1), since the front moved eastwards much faster than onshore waters ($\Delta\mu X_{on}$ = 5.7 cm s^{-1}; Table 1).

Front 4 showed the clearest signs of convergence. Both offshore and onshore drifters converged at the front, moving with speeds of 8.3 ± 0.4 cm s^{-1} and −3.5 ± 0.2 cm s^{-1}, respectively, while the front approached the coast at 2 ± 0.4 cm s^{-1} (Table 1, Fig. 4). This was the only front with positive net convergence speeds from the offshore side of the front ($\Delta\mu Y_{off} > 0$; Table 1). Drifter trajectories revealed a prevailing eastward flow, which was more intense at the front (μX_{f} = 8.2 ± 0.8 cm s^{-1}) than on either side of the convergence. Waters subducted at the front, especially from the onshore side ($\Delta\mu Z_{on}$ = −9.6 cm s^{-1}).

Meroplankton distribution

We found high larval diversity in terms of species, developmental stages and locomotion abilities (Table 2). Swimming velocities of the larvae in our study varied greatly depending on taxon, from slow veligers to cyprids that can cover 90 times their body length per second (Anderson 1992; our Table 2). In addition, the taxonomic composition of the larval community and the spatial distributions around the fronts were clearly different among the 4 fronts (Fig. 5).

Fast-swimming zoeae of *Pachygrapsus marmoratus* and *Chthamalus* spp. cyprids showed a clear accumulation pattern at Front 1 (Fig. 5), likely originating at the onshore side, since $\Delta\mu Y_{off}$ was negative (Table 1). Slower chrysopetalid annelid segmented larvae and *Chthamalus* spp. early and late nauplii aggregated offshore (Fig. 5). No significant pattern was found for littorinid veligers (Fig. 5).

Front 2 had no significant effect on the distribution of any larvae (Fig. 5). Although ascidian larvae seemed to be concentrated in the front, their relatively high mean abundance at the convergence was based on only 1 sample.

In Front 3, fast-swimming cyprids of *Perforatus perforatus* and *Chthamalus* spp. were most abundant in onshore and frontal waters (Fig. 5), and slower chrysopetalid segmented larvae and littorinid veligers accumulated at the front (Fig. 5). As in Front 1, accumulating larvae were likely supplied from the onshore side of the front, since the velocity of the offshore surface waters was negative with respect to the front ($\Delta\mu Y_{off} < 0$; Table 1). *Membranipora* spp. cyphonauts did not show a significant pattern (Fig. 5).

In Front 4, slow ascidian tadpole larvae accumulated (Fig. 5), with a higher supply rate from the onshore than the offshore side of the front (Table 3). Faster *Chthamalus* spp. cyprids also accumulated at the front (Fig. 5), but their origin was probably offshore of the front (Table 3). Despite their different

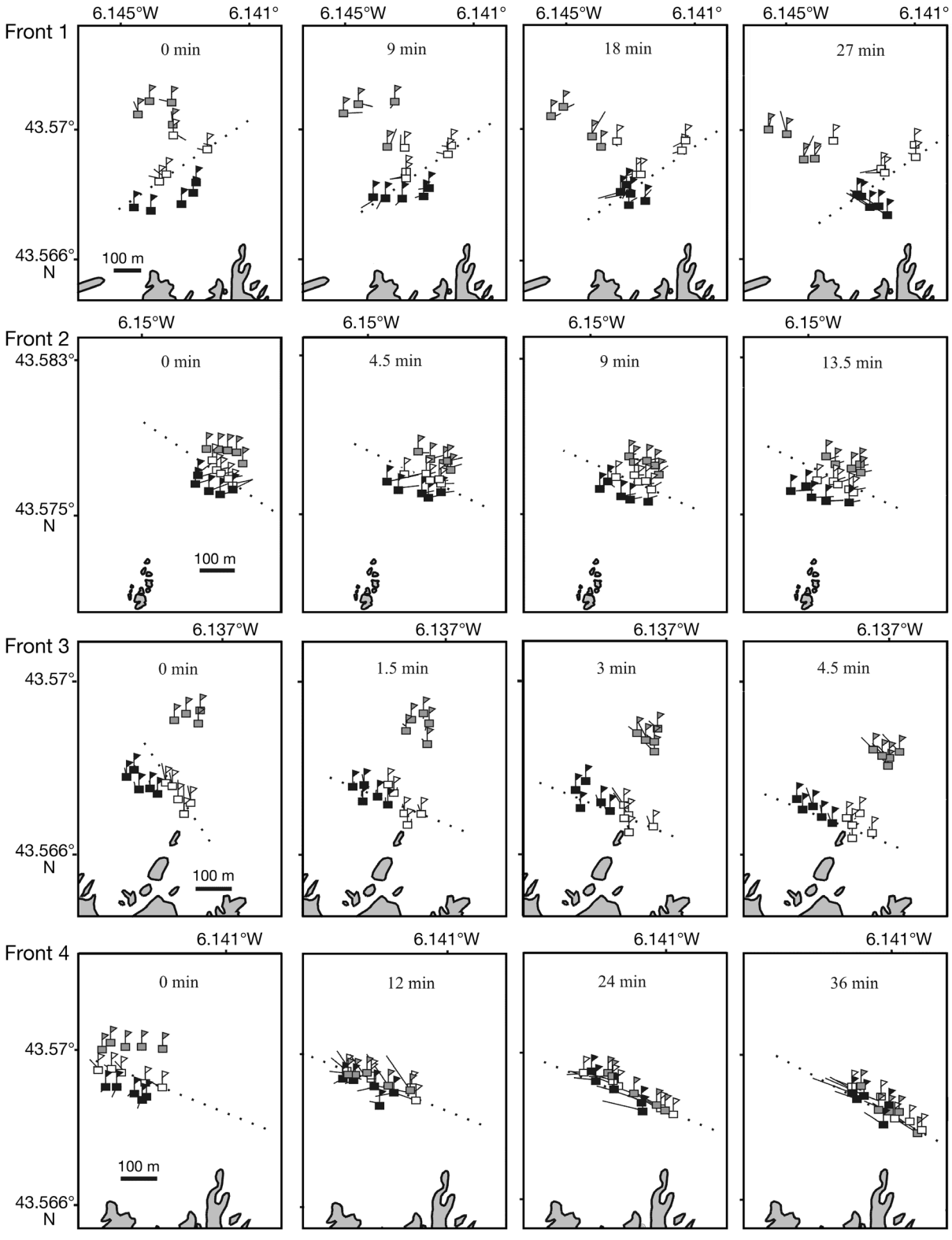

Fig. 4. Trajectories of onshore (black), frontal (white) and offshore (grey) drifters. Time intervals of 9, 4.5, 1.5 and 12 min were used to represent drifter movements for Fronts 1 to 4, respectively. Dark lines attached to the flags show the distance covered during each time interval (note that at Time 0, frontal and onshore drifters for Fronts 2 to 4 and frontal and offshore drifters for Front 1 indicate a distance already covered since they were the first to be deployed). Dotted lines mark the approximate position of the front according to *in situ* observation

Table 2. Published larval swimming velocities (μ_l)

Taxon	μ_l (cm s^{-1})	Reference
Perforatus perforatus cyprids	6.7	Anderson (1994)
Chthamalus spp. cyprids	5.7	Anderson (1994)
Pachygrapsus marmoratus zoeae	2.2	Knudsenj (1960), Chia et al. (1984)
Chrysopetalids	0.7	Nozais et al. (1997)
Chthamalus spp. late nauplii	0.4	Williams (1994), Walker (2004)
Ascidians	0.3	McHenry (2005)
Perforatus perforatus early nauplii	0.3	Williams (1994), Walker (2004)
Verruca stroemia early nauplii	0.3	Williams (1994), Walker (2004)
Chthamalus spp. early nauplii	0.3	Williams (1994), Walker (2004)
Littorinid veligers	0.13	Mileikovsky (1973), Chia et al. (1984)
Membranipora spp.	0.11	Abelson (1997)

swimming velocities, cyprids of *Perforatus perforatus*, zoeae of *Pachygrapsus marmoratus* and early nauplii of *Perforatus perforatus, Verruca stroemia* and *Chthamalus* spp. were more abundant onshore and at the front than on the offshore side of the front (Fig. 5).

Source of accumulated larvae

The source of larvae found at the slicks could be clearly identified as onshore waters in 3 out of 4 fronts because $\Delta\mu Y_{off} < 0$ (Tables 1 & 3). The situation was less clear for Front 4, where both $\Delta\mu Y_{off}$ and $\Delta\mu Y_{on}$ were positive (Tables 1 & 3). In this case, we only consider the comparison between supply rates in those taxa that significantly accumulated in the front (see 'Materials and methods: Data analysis'). Thus, ascidian tadpole larvae had a higher contribution from onshore waters, while in *Chthamalus* spp. cyprids an offshore origin prevailed (Table 3). Once the source of larvae and their speed were known for the available taxa at each event, both accumulation and cross-frontal velocity ratios (A and Q_Y) were calculated and $\log(A)$ was plotted as a function of $\log(Q_Y)$ (Fig. 6A); the least-squares fit to a quadratic equation is:

$$\log(A) = -0.60\,[\log(Q_Y)]^2 - 0.49\log(Q_Y) + 0.70 \quad (8)$$

where coefficients have standard errors of ±0.20, ±0.20 and ±0.21, respectively, and $R^2 = 0.40$, $p = 0.025$ and $n = 17$ (Fig. 6A). The same procedure was followed using the vertical velocity ratio Q_Z:

$$\log(A) = -0.69\,[\log(Q_Z)]^2 - 1.16\log(Q_Z) + 0.28 \quad (9)$$

where coefficients have standard errors of ±0.31, ±0.47 and ±0.23, respectively, and $R^2 = 0.30$, $p = 0.08$ and $n = 17$ (Fig. 6B). In addition, to investigate the relationship between both larval velocity ratios, $\log(Q_Z)$ and $\log(Q_Y)$ were correlated using a simple linear fit:

$$\log(Q_Z) = 0.83\log(Q_Y) - 0.43 \quad (10)$$

where coefficients have standard errors of ±0.08 and ±0.08, respectively, and $R^2 = 0.87$, $p < 0.0001$ and $n = 17$ (Fig. 6C).

DISCUSSION

Physical structure of surface convergences

On 4 occasions during a 10 d period, we sampled foam lines observed from shore prior to dissipation of the foam line and surface convergence, which typically occurred in a matter of hours (suggesting tidal or diel mechanisms). Irrespective of the origin of the surface convergence, we observed larval accumulation whenever we observed convergent flow with surface drifters (summarized in Fig. 6). Surface convergences may form at fronts due to surface plumes (e.g. Nalón River), upwelling (east winds) and internal waves, and along flow separation lines (Le Fevre 1986, Longhurst 1998, Pineda 1999, Shanks et al. 2000, McCulloch & Shanks 2003). Without a more complete set of physical data, we cannot confidently attribute the 4 observed features to a specific physical process, but the diversity in structure and imputed mechanism may not be a critical factor to explain larval spatial patterns as long as there is a convergent surface flow driving larval transport and accumulation.

Although it may not be possible to define the specific physical processes responsible for frontal development, each front was characterized by different hydrographical and meteorological features. The density structure at the time we sampled Front 1 was dominated by the salinity structure, although the front was displaced from the location of the strongest salinity gradient (possibly, the salinity front was immediately offshore of the station at ~700 m, and the foam line indicating the front was displaced

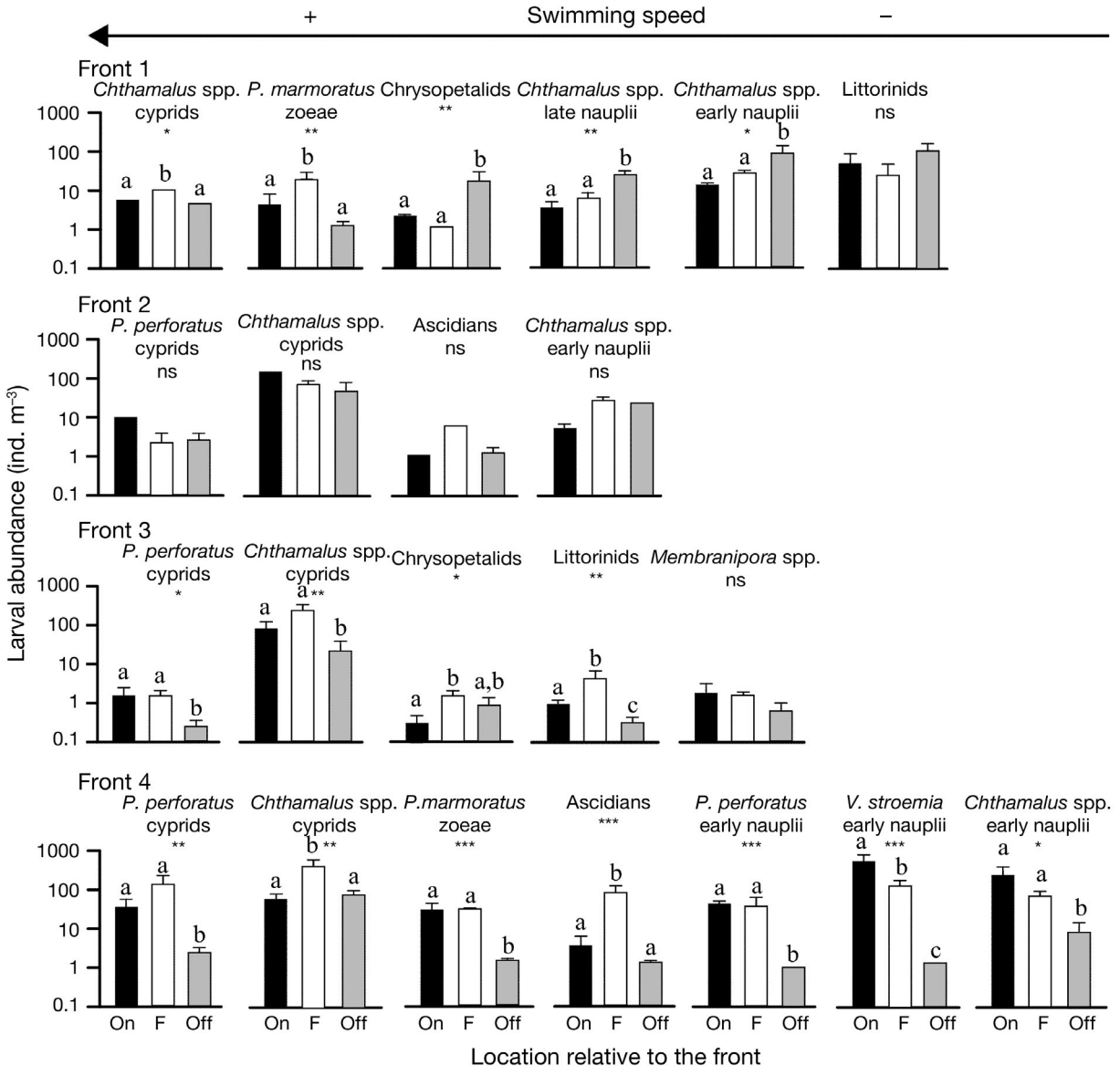

Fig. 5. Mean larval densities (+SD) onshore (black bar), at the front (white), and offshore (grey). Panels for each larval taxon are arranged from left to right according to their swimming velocities (Table 2). Results of the ANOVA analysis: *p < 0.05, **p < 0.01, ***p < 0.001, ns = not significant. Bars sharing lower case letters are not significantly different according to a Fisher's post hoc test

200 m towards the shore by the sea breeze). Near-surface thermal structure near the foam line resulted in negligible density structure and was considered inadequate to drive convergence and subduction. Thus, this foam line (and additional foam lines at 700 m and 1200 m offshore) may have marked the inshore edge of the low-salinity waters associated with Nalón outflow. However, the landward intrusion of cool, high-fluorescence waters at depth suggests an internal wave run-up, which may have had an additional role in the formation of the surface convergence (although there was imperceptible density structure associated with this feature at the time of sampling; Fig. 3). For Front 3, winds were weak and density structure was dominated by salinity as was the case for Front 1, but with the difference of a shallow, warm, low-salinity lens in the vicinity of the front — again suggesting influences from the Nalón plume (Figs. 2 & 3). We observed colder waters at depth and a subsurface chlorophyll maximum, which is consistent with recent upwelling a day earlier (Fig. 2) and upwelled waters now capped by the warm, low-salinity layer. In contrast, Front 2 was observed during upwelling winds (Fig. 2). Its density structure correlated with both temperature and salinity, and cooler waters were breaking the surface

Table 3. Larval supply rates to the front (S_{on} and S_{off}, depending on whether the presumed source is the onshore or the offshore side of the front, ind. m^{-2} s^{-1}), and the accumulation ratio (A, non-dimensional) for each combination of larval taxa and front. The source of the larvae could only be inferred for those taxa that accumulated significantly in Front 4, while offshore supply rates could not be calculated when offshore cross-frontal velocities were negative (na = not applicable; see 'Material and methods: Data analysis'). Larval taxa have been arranged according to their swimming velocity (see Table 2)

Taxon	S_{on}	S_{off}	Source	A
Front 1				
Chthamalus spp. cyprids	0.41	na	Onshore	2.27
Pachygrapsus marmoratus zoeae	0.26	na	Onshore	5.39
Chrysopetalids	0.08	na	Onshore	0.1
Chthamalus spp. late nauplii	0.19	na	Onshore	2.06
Chthamalus spp. early nauplii	1.10	na	Onshore	2.12
Littorinid veligers	3.85	na	Onshore	0.52
Front 2				
Perforatus perforatus cyprids	0.04	na	Onshore	0.13
Chthamalus spp. cyprids	0.78	na	Onshore	0.44
Chthamalus spp. early nauplii	0.02	na	Onshore	6.49
Ascidians	0.0006	na	Onshore	43.37
Front 3				
Perforatus perforatus cyprids	0.20	na	Onshore	0.97
Chthamalus spp. cyprids	11.69	na	Onshore	2.95
Chrysopetalids	0.02	na	Onshore	7.75
Littorinid veligers	0.11	na	Onshore	5.15
Membranipora spp.	0.23	na	Onshore	0.95
Front 4				
Perforatus perforatus cyprids	1.78	0.09	na	na
Chthamalus spp. cyprids	3.11	4.79	Offshore	5.87
Pachygrapsus marmoratus zoeae	1.55	0.01	na	na
Chthamalus spp. early nauplii	12.67	0.49	na	na
Perforatus perforatus early nauplii	2.18	0	na	na
Verruca stroemia early nauplii	29.03	0.02	na	na
Ascidians	0.13	0.01	Onshore	30.26

nearshore (Fig. 3). We sampled Front 2 during the daily minimum in wind forcing, perhaps as upwelling started to relax — a time when surface fronts may develop and propagate shoreward (cf. Shanks et al. 2000). Sampling of Front 4 indicated the absence of a density structure that could have accounted for the observed surface convergence, although an intrusion of low-salinity waters may have been entrained along the front (Fig. 3; cf. Graham & Largier 1997). This absence of density structure along with

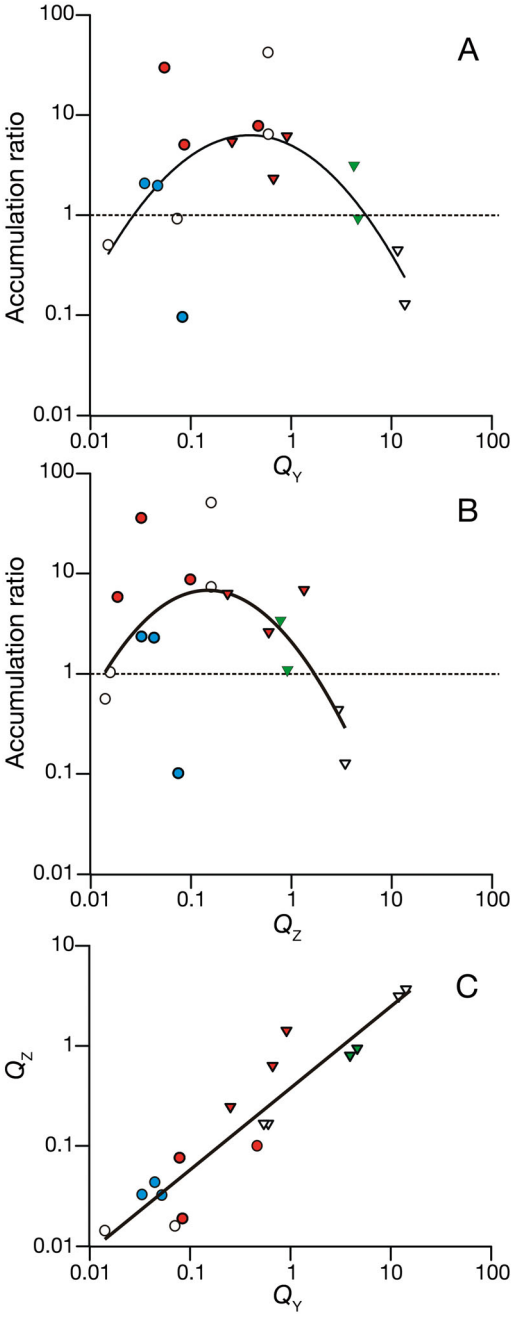

Fig. 6. Relationship (A) between accumulation ratio (A, number of larvae in the front per number of larvae at the source) and velocity quotient Q_Y (larval velocities divided by the cross-frontal flow), (B) between A and Q_Z (larval velocities divided by the vertical flows), and (C) between Q_Z and Q_Y. Each data point corresponds to a combination of larval taxon and front; circles: slow larvae ($\mu_l < 1$ cm s^{-1}); triangles: fast larvae ($\mu_l > 1$ cm s^{-1}) (see Table 2). Curves in (A) and (B) indicate the least-squares fit of the log-transformed data to a second order polynomial (n = 17; Eqs. 8 & 9). In (C), the straight line represents the least-squares linear fit (n = 17, Eq. 10). Colours indicate distribution patterns as detected by ANOVA — blue: offshore aggregation; red: frontal accumulation; green: onshore aggregation; white: no significant pattern (Table 3, Fig. 5)

the width of the foam line and the amount of floating debris suggests that Front 4 was a result of separation of eastward flow at the point/ridge offshore and west of Cudillero Harbour (Fig. 1). As flow reaches the separation point, it likely curves (cf. McCabe et al. 2006), converging on the separation foam line past the point.

Spatial distribution of larvae around coastal fronts

Our results agree with other studies reporting accumulation of crustaceans, polychaetes and gastropods at nearshore fronts and slicks (Zeldis & Jillet 1982, Shanks 1995, Pineda 1999, Molinet et al. 2006). In addition, we detected accumulation of ascidian larvae at these slicks (Fig. 5). Our maximum observed accumulation ratios (Fig. 6) were higher than prior model predictions (e.g. less than 2 larvae at the front per larva at the source, as suggested by Lennert-Cody & Franks 1999). Accumulation ratios were particularly high for ascidian tadpole larvae (Table 3), probably because they are positively buoyant like ascidian eggs (Vázquez & Young 1996). Upward swimming against downward frontal flows has already been observed in mero- and zooplankton (Genin et al. 2005, Shanks & Brink 2005) and is likely responsible for observed larval accumulation (Franks 1992, Pineda 1999). With the exception of Front 4, our data suggest that larvae accumulated from the onshore side of fronts (Table 3). Thus, in addition to accumulation, fronts may also cause onshore retention, as already suggested by theoretical advection-diffusion models and observations on larval distributions in other areas (Cowen 2000, Mace & Morgan 2006). In essence, the fronts would sweep larvae located in the nearshore surface waters towards the coast, with consecutive strokes in the case of series of internal waves.

Accumulation model

The conceptual model underlying the observed statistical model (Eq. 5, Fig. 6A) is based on 2 assumptions: (1) organisms that swim much slower than the observed cross-frontal surface convergence ($0.01 < Q_Y < 0.1$) will follow streamlines and be carried offshore from the front in a sub-surface divergence that counter-balances the observed surface convergence (Franks 1992, Shanks et al. 2000), and (2) organisms that swim much faster than the cross-frontal surface velocity convergence ($1 < Q_Y < 10$) will not be constrained by the feature, thus retaining their original onshore distribution patterns close to their source on the intertidal and shallow sub-tidal. Both assumptions are confirmed by the fact that onshore and offshore larval aggregations were found at high and low values of the cross-frontal velocity ratio, respectively (Fig. 6A). While individual points are notably scattered (Fig. 6A), the relationship between accumulation ratio (A) and Q_Y indicated by Eq. (8) is significant ($p = 0.025$). Further, the relationship is only expected to be meaningful for positive accumulations greater than 1, and the model becomes more convincing when one notes that $A > 1$ only for intermediate swimming speeds ($0.05 < Q_Y < 8$) and that there are no negative results ($A < 1$) for a similar range of swimming speeds ($0.09 < Q_Y < 10$). Lastly, the fundamental concept of optimum frontal accumulation at intermediate swimming speeds remains statistically significant for any selection of 16 data points (the result does not depend on any single data point).

The unimodal curve is similar yet less clear when swimming speed in relation to the vertical flow (Q_Z) is considered instead of Q_Y (Fig. 6B). The quadratic fit is no longer significant although it accounts for up to 30% of the total variability in A (Fig. 6B). Similar patterns of variation in A with both relative swimming velocities are expected, since Q_Y and Q_Z are correlated (Fig. 6C). This linear correlation is also expected, as both velocity quotients were calculated using the same larval swimming speeds (Table 2), and the vertical and cross-frontal flows may be related (Table 1). Surprisingly, the vertical flow was slightly stronger than the horizontal cross-shore convergence (Table 1), whereas direct measurements in the ocean have indicated that vertical currents are 10 or even 100 times slower (Rodriguez et al. 2001, Manasrah et al. 2006). These slow vertical currents may be faster around fronts in convergent systems as water is forced downwards. Calculating the magnitude of vertical currents depends on the ratios H/W and H/L which could be lower than 1 (see Eq. 5). Thus, the vertical:horizontal ratio may vary between 1:10 or lower for weaker fronts (Yanagui et al. 1995) to 1:1 for the Columbia River plume front with vertical currents up to 0.5 m s^{-1} (Kilcher & Nash 2010). Due to the stronger vertical flow calculated in our study, theoretical ability of larvae to withstand the currents decreases in this axis: Q_Z is lower than Q_Y, and the slope of the linear fit between both is smaller than unity (Eq. 10, Fig. 6C). Consequently, those values of the horizontal ratio at which frontal accumulation was observed ($0.05 < Q_Y < 8$) may correspond to

lower ranges of the vertical ratio Q_Z (Fig. 6A,B). These observations lead to a paradox: how can frontal accumulation develop if the horizontal, cross-frontal flow that brings larvae to the convergence is weaker than the vertical currents that may potentially remove those larvae from it? This apparent contradiction may be resolved by recognizing the aspect ratio of the frontal flow $H/W < 1$, or by recognizing that larval ability to face the currents in the vertical axis may be enhanced by buoyancy and active swimming behaviour. Field observations and theoretical models have showed that vertical buoyancy has the same importance as swimming ability in the aggregation of organisms at propagating fronts (Helfrich & Pineda 2003). In addition, Genin et al. (2005) demonstrated at 2 coastal sites that even when vertical and horizontal currents were of the same magnitude, zooplankton passively drifted horizontally but actively swam against the vertical flow. Such a behavioural strategy may lead to very efficient horizontal transport of larvae towards the front, possibly concealing larval losses driven by strong frontal subduction.

While our data strongly support this conceptual model of frontal accumulation, several factors affecting larval biology and physical structure of coastal fronts need further analysis. (1) Despite some extensive reviews (Mileikovsky 1976, Chia et al. 1984), larval swimming speeds are not well known. (2) We know little about the variability in swimming speed within a population of invertebrate larvae, which would affect the probability of larval accumulation at a front. (3) Our vertical flow values are just rough estimates obtained using a simple mass balance assumption. (4) These estimates show that frontal circulation does not necessarily lead to subduction at the front: note that for Front 2, when along-frontal velocities were considered, vertical speeds were directed slightly upwards (Table 1). In such a case, swimming against the vertical flow may not drive frontal accumulation, but larval losses. Unfortunately, as the onshore cross-frontal flow was quite weak in Front 2 (0.5 cm s^{-1}; Table 1), larvae may not even have reached the front in significant numbers and therefore did not accumulate (Fig. 5); therefore, it is rather difficult to draw any conclusions from this particular event. (5) Ideally frontal convergence and accumulation should be tracked for an extended period, since accumulation is the product of convergence rate and persistence of the convergence feature over a period of time. Even if the convergence process has already dissipated, one may still observe an associated accumulation (e.g. Front 2). (6) The fact that fronts were likely sampled during different stages of development and that stations were not interspersed may have led to confounding effects. In spite of these uncertainties, our results strongly support the model of larval accumulation due to convergent surface flow.

According to Fig. 6, slow (mm s^{-1}) and fast (cm s^{-1}) larvae presented low and high relative velocities, respectively. This segregation is particularly evident in Fig. 6C, where fast swimmers fall within domains defined by high values of Q_Y and Q_Z, while the opposite is true for slow swimmers. This suggests that the ranges of possible velocity quotients are limited, since both the range of current velocities in the ocean and the speed of a given organism are limited. Such a constraint may be evident for those species attaining extreme swimming speeds. Considering the quadratic fit obtained with Q_Y, barnacle cyprids, which swim at $\mu_l > 5$ cm s^{-1} (Table 2), would require a convergent flow velocity of at least 2 m s^{-1} to achieve relative cross-frontal speeds leading to offshore aggregation ($Q_Y < 0.05$). This flow velocity is faster than the maximum surface current velocities measured in this area (i.e. ca. 1 m s^{-1}, ADCP [acoustic Doppler current profiler] data from October 2008 to April 2009; Fig. 1). In contrast, weak, slow swimmers attaining speeds of only a few mm s^{-1} (Table 2) would require a null convergent flow (<0.1 mm s^{-1}) to achieve Q_Y values typical of onshore aggregation patterns ($Q_Y > 5$). In essence, under the physical forcing of coastal fronts, slow swimmers would not remain inshore and fast larvae would not be transported offshore. Only at moderate larval speeds ($0.7 < \mu_l < 3$ cm s^{-1}) are all the spatial patterns around the slick theoretically possible.

Stage-specific frontal effects and potential recruitment

Our work points to the potential of fronts to generate spatial population dislocations (sensu Franks 1992), i.e. a segregation of the planktonic communities according to the swimming abilities of the different species. These segregations were especially evident in Front 1 and affected not only distributions of different species but also of life history stages within species. This was the case for the barnacles *Chthamalus* spp., whose slow-swimming nauplii had an offshore distribution, while the fast-swimming cyprids accumulated at the slick (Fig. 5). Thus, the same physical process disperses the early larval phases offshore while bringing the competent, cyprid stage inshore. These observations are coincident

with those of Tapia & Pineda (2007), who reported stage-specific cross-shore distributions in *Chthamalus* spp., probably driven by active larval swimming behaviour.

Three out of 4 fronts moved inshore, reached the shoreline and accumulated competent barnacle and/or littorinid larvae (Fig. 5), thus their role in recruitment may be important. Although post-settlement processes entailing high mortality rates may affect population dynamics to a greater extent and thus may conceal potential inputs of new recruits provided by the slicks (Largier 2003), mesoscale studies along the Eastern Pacific coast successfully link slick occurrence with high recruitment rates for different species (Lagos et al. 2008, Woodson et al. 2012).

CONCLUSIONS

In summary, our study shows that nearshore fronts may greatly affect larval distributions in their surroundings. They provide larval retention by accumulating larvae from inshore waters, but their effects depend largely on specific larval swimming performance relative to vertical currents and, especially, relative to the cross-frontal, horizontal flow. This interaction between environmental and organismal velocities determines the spatial distribution of larvae around coastal convergences. Our estimates indicate a strong vertical flow at the front and suggest that other characteristics such as buoyancy and behavioural shifts in swimming activity may also be relevant to explain frontal larval accumulation. Further work should provide measurements of both vertical and horizontal currents and estimates of plankton abundances at different depths, in combination with concurrent direct estimations of larval recruitment to the intertidal habitat, to fully appreciate the 3-dimensional nature of these hydrographic structures.

Acknowledgements. We thank A. Prada and C. Cáceres for assistance onboard RV 'Nueva Asturias'. R. Anadón, F. González-Taboada and J. Arrontes improved the manuscript with their comments. We are indebted to S. Weidberg, T. Weidberg and J. Weidberg for improving the text. Thanks to an anonymous reviewer for comments that led to improved revision. Meteorological data sets were kindly provided by Puertos del Estado, Spanish Ministry of Public Works. This research was funded by projects COSTAS (CTM2006-05588/MAR, Ministry of Education and Science, Spanish Government) and FRENTES (IB08-122, FICYT, Government of the Principality of Asturias). This is a contribution of the Asturian Marine Observatory.

LITERATURE CITED

Abelson A (1997) Settlement in flow: upstream exploration of substrata by weakly swimming larvae. Ecology 78: 160–166

Anderson DT (1994) Larval development and metamorphosis. In: Anderson DT (ed) Barnacles: structure, function, development and evolution. Chapman & Hall, London, p 197–239

Archambault P, Bourget E (1999) The influence of shoreline configuration on spatial variation of meroplanktonic larvae, recruitment and diversity of benthic subtidal communities. J Exp Mar Biol Ecol 238:161–186

Bakun A (1973) Coastal upwelling indices, west coast of North America, 1946–71. NOAA Technical Report NMFS SSRF-671. US Department of Commerce, Seattle, WA

Becker BJ, Levin LA, Fodrie FJ, McMillan PA (2007) Complex larval connectivity patterns among marine invertebrate populations. Proc Natl Acad Sci USA 104: 3267–3272

Chia FS, Buckland-Nicks J, Young CM (1984) Locomotion of marine invertebrate larvae: a review. Can J Zool 62: 1205–1222

Cowen RK, Lwiza KMM, Sponaugle S, Paris CB, Olson DB (2000) Connectivity of marine populations: open or closed? Science 287:857–859

Franks PJS (1992) Sink or swim: accumulation of biomass at fronts. Mar Ecol Prog Ser 82:1–12

Gaines S, Roughgarden J (1985) Larval settlement rate: a leading determinant of structure in an ecological community of the marine intertidal zone. Proc Natl Acad Sci USA 82:3707–3711

Gallager SM, Yamazaki H, Cabell S, Davis CS (2004) Contribution of fine-scale vertical structure and swimming behavior to formation of plankton layers on Georges Bank. Mar Ecol Prog Ser 267:27–43

Genin A, Jaffe SJ, Reef R, Richter C, Franks PJS (2005) Swimming against the flow: a mechanism of zooplankton aggregation. Science 308:860–862

Graham WM, Largier JL (1997) Upwelling shadows as nearshore retention sites: the example of northern Monterey Bay. Cont Shelf Res 17:509–532

Guichard F, Bourget E (1998) Topographic heterogeneity, hydrodynamics, and benthic community structure: a scale-dependent cascade. Mar Ecol Prog Ser 171:59–70

Helfrich KR, Pineda J (2003) Accumulation of particles in propagating fronts. Limnol Oceanogr 48:1509–1520

Kilcher LF, Nash DJ (2010) Structure and dynamics of the Columbia River tidal plume front. J Geophys Res 115: C05S90, doi:10.1029/2009JC006066

Kingsford MJ, Choat JH (1986) Influence of surface slicks on the distribution and onshore movements of small fish. Mar Biol 91:161–171

Knudsen JW (1960) Reproduction, life history, and larval ecology of the California Xanthidae, the pebble crabs. Pac Sci 14:3–17

Lagos NA, Castilla JC, Broitman BR (2008) Spatial environmental correlates of intertidal recruitment: a test using barnacles in Northern Chile. Ecol Monogr 78: 245–261

Largier JL (1993) Estuarine fronts: How important are they? Estuaries 16:1–11

Largier JL (2002) Linking oceanography and nearshore ecology: perspectives and challenges. In: Castilla JC, Largier JL (eds) The oceanography and ecology of the

nearshore and bays in Chile. Proceedings of the International Symposium on Linkages and Dynamics of Coastal Systems: Open Coast and Embayments, Santiago, p 207–239

Largier JL (2003) Considerations in estimating larval dispersal distances from oceanographic data. Ecol Appl 13(Suppl):S71–S89

Le Fevre J (1986) Aspects of the biology of frontal systems. 1st edn. Université de Bretagne Occidentale, Brest

Leichter JJ, Shellenbarger G, Genovese JS, Wing SR (1998) Breaking internal waves on a Florida (USA) coral reef: a plankton pump at work? Mar Ecol Prog Ser 166:83–97

Lennert-Cody CE, Franks PJS (1999) Plankton patchiness in high-frequency internal waves. Mar Ecol Prog Ser 186: 59–66

Longhurst A (1998) Ecological geography of the sea. 1st edn. Academic Press, San Diego, CA

Luckenbach MW, Orth RJ (1992) Swimming velocities and behavior of blue crab (*Callinectes sapidus* Rathbun) megalopae in still and flowing water. Estuaries 15: 186–192

Mace AJ, Morgan SG (2006) Biological and physical coupling in the lee of a small headland: contrasting transport mechanisms for crab larvae in an upwelling region. Mar Ecol Prog Ser 324:185–196

Magome S, Yamashita T, Kohama T, Kaneda A, Hayami Y, Takahashi S, Takeoka H (2007) Jellyfish patch formation investigated by aerial photography and drifter experiment. J Oceanogr 63:761–773

Manasrah RS, Al-Horani FA, Rasheed MY, Al-Rousan SA, Khalaf MA (2006) Patterns of summer vertical and horizontal currents in coastal waters of the northern Gulf of Aqaba, Red Sea. Estuar Coast Shelf Sci 69:567–579

Mann R (1988) Distribution of bivalve larvae at a frontal system in the James River, Virginia. Mar Ecol Prog Ser 50: 29–44

McCabe RM, MacCready P, Pawlak G (2006) Form drag due to flow separation at a headland. J Phys Oceanogr 36: 2136–2152

McCulloch A, Shanks AL (2003) Topographically generated fronts, very nearshore oceanography and the distribution and settlement of mussel larvae and barnacle cyprids. J Plankton Res 25:1427–1439

McHenry MJ (2005) The morphology, behavior, and biomechanics of swimming in ascidian larvae. Can J Zool 83: 62–74

Metaxas A (2001) Behaviour in flow: perspectives on the distribution and dispersion of meroplanktonic larvae in the water column. Can J Fish Aquat Sci 58:86–98

Mileikovsky SA (1973) Speed of active movement of pelagic larvae of marine bottom invertebrates and their ability to regulate their vertical position. Mar Biol 23:11–17

Molinet C, Valle-Levinson A, Moreno AC, Cáceres M, Bello M, Castillo M (2006) Effects of sill processes on the distribution of epineustonic competent larvae in a stratified system of Southern Chile. Mar Ecol Prog Ser 324:95–104

Nozais C, Duchke JC, Bhaud M (1997) Control of position in the water column by the larvae of *Poecilochaetus serpens* (Polychaeta): the importance of mucus secretion. J Exp Mar Biol Ecol 210:91–106

Pineda J (1999) Circulation and larval distribution in internal tidal bore warm fronts. Limnol Oceanogr 44: 1400–1414

Pineda J, López M (2002) Temperature, stratification and barnacle larval settlement in two Californian sites. Cont Shelf Res 22:1183–1198

Pineda J, Hare JA, Sponaugle S (2007) Larval transport and dispersal in the coastal ocean and consequences for population connectivity. Oceanography (Wash DC) 20:22–39

Pineda J, Reyns NB, Starczak VR (2009) Complexity and simplifications in understanding recruitment in benthic populations. Popul Ecol 51:17–32

Poulin E, Palma AT, Leiva G, Hernández E, Martinez P, Navarrete SA, Castilla JC (2002) Temporal and spatial variation in the distribution of epineustonic competent larvae of *Concholepas concholepas* along the central coast of Chile. Mar Ecol Prog Ser 229:95–104

Rodríguez J, Tintoré J, Allen JT, Blanco JM and others (2001) Mesoscale vertical motion and the size structure of phytoplankton in the ocean. Nature 410:360–363

Rodríguez JM, González-Pola C, López-Urrutia A, Nogueira E (2011) Composition and daytime vertical distribution of the ichthyoplankton assemblage in the Central Cantabrian Sea shelf, during summer: an Eulerian study. Cont Shelf Res 31:1462–1473

Sameoto D, Wiebe P, Runge J, Postel L, Dunn J, Miller C, Coombs S (2000) Collecting zooplankton. In: Harris R, Wiebe P, Lenz J, Skjoldal HR, Huntley M (eds) ICES zooplankton methodology manual. 1st edn. Academic Press, London, p 55–78

Sandifer P (1975) The role of pelagic larvae in recruitment to populations of adult decapod crustaceans in the York River estuary and adjacent lower Chesapeake Bay, Virginia. Estuar Coast Mar Sci 3:269–279

Scotti A, Pineda J (2007) Plankton accumulation and transport in propagating nonlinear internal fronts. J Mar Res 65:117–145

Shanks AL (1995) Orientated swimming by megalopae of several eastern North Pacific crab species and its potential role in their onshore migration. J Exp Mar Biol Ecol 186:1–16

Shanks AL, Brink L (2005) Upwelling, downwelling, and cross-shelf transport of bivalve larvae: test of a hypothesis. Mar Ecol Prog Ser 302:1–12

Shanks AL, Largier J, Brink L, Brubaker J, Hoof R (2000) Demonstration of the onshore transport of larval invertebrates by the shoreward movement of an upwelling front. Limnol Oceanogr 45:230–236

Shanks AL, Largier JL, Brink L, Brubaker J, Hoof R (2002) Observations on the distribution of meroplankton during a downwelling event and associated intrusion of the Cheseapeake Bay estuarine plume. J Plankton Res 24: 391–416

Shanks AL, McCulloch A, Miller J (2003) Topographically generated fronts, very nearshore oceanography and the distribution of larval invertebrates and holoplankters. J Plankton Res 25:1251–1277

Tapia F, Pineda J (2007) Stage specific distribution of barnacle larvae in nearshore waters: potential for limited dispersal and high mortality rates. Mar Ecol Prog Ser 342: 177–190

Vázquez E, Young CM (1996) Responses of compound ascidian larvae to haloclines. Mar Ecol Prog Ser 133: 179–190

Walker G (2004) Swimming speeds of the larval stages of the parasitic barnacle *Heterosaccus lunatus*. J Mar Biol Assoc UK 84:737–742

Weidberg N, Acuña JL, Lobón C (2013) Seasonality and fine-scale meroplankton distribution off the central Cantabrian Coast. J Exp Mar Biol Ecol 442:47–57

Williams TA (1994) The nauplius larva of crustaceans: functional diversity and the phylotypic stage. Am Zool 34: 562–569

Wolanski E, Imberger J, Heron M (1984) Island wakes in shallow coastal waters. J Geophys Res 89:10553–10569, doi:10.1029/JC089iC06p10553

Woodson CB, McManus MA, Tyburczy JA, Barth JA and others (2012) Coastal fronts set recruitment and connectivity patterns across multiple taxa. Limnol Oceanogr 57: 582–596

Young M, Adams NJ (2010) Plastic debris and seabird presence in the Hauraki Gulf, New Zealand. NZ J Mar Freshw Res 44:167–175

Zeldis JR, Jillet JB (1982) Aggregation of pelagic *Munida gregaria* (Fabricius) (Decapoda, Anomura) by coastal fronts and internal waves. J Plankton Res 4: 839–857

Editorial responsibility: Paul Snelgrove, St. John's, Newfoundland and Labrador, Canada

Submitted: October 2, 2013; Accepted: March 2, 2014
Proofs received from author(s): May 21, 2014